

Article

Natural Background Levels of Potentially Toxic Elements in Groundwater from a Former Asbestos Mine in Serpentinite (Balangero, North Italy)

Elisa Sacchi ^{1,*}, Massimo Bergamini ², Elisa Lazzari ², Arianna Musacchio ¹, Jordi-René Mor ¹ and Elisa Pugliaro ²

¹ Department of Earth and Environmental Sciences, University of Pavia, Via Ferrata 9, I-27100 Pavia, Italy; arianna.musacchio01@universitadipavia.it (A.M.); jrene.mor@irsa.cnr.it (J.-R.M.)

² R.S.A. Srl, Viale Copperi 15, I-10070 Balangero, Italy; bergamini@rsa-srl.it (M.B.); lazzari@rsa-srl.it (E.L.); pugliaro@rsa-srl.it (E.P.)

* Correspondence: elisa.sacchi@unipv.it; Tel.: +39-0382-985880

Abstract: The definition of natural background levels (NBLs) for potentially toxic elements (PTEs) in groundwater from mining environments is a real challenge, as anthropogenic activities boost water–rock interactions, further increasing the naturally high concentrations. This study illustrates the procedure followed to derive PTE concentration values that can be adopted as NBLs for the former Balangero asbestos mine, a “Contaminated Site of National Interest”. A full hydrogeochemical characterisation allowed for defining the dominant Mg-HCO₃ facies, tending towards the Mg-SO₄ facies with increasing mineralisation. PTE concentrations are high, and often exceed the groundwater quality thresholds for Cr VI, Ni, Mn and Fe (5, 20, 50 and 200 µg/L, respectively). The Italian guidelines for NBL assessment recommend using the median as a representative concentration for each monitoring station. However, this involves discarding half of the measurements and in particular the higher concentrations, thus resulting in too conservative estimates. Using instead all the available measurements and the recommended statistical evaluation, the derived NBLs were: Cr = 39.3, Cr VI = 38.1, Ni = 84, Mn = 71.36, Fe = 58.4, Zn = 232.2 µg/L. These values are compared to literature data from similar hydrogeochemical settings, to support the conclusion on their natural origin. Results highlight the need for a partial rethink of the guidelines for the assessment of NBLs in naturally enriched environmental settings.



Citation: Sacchi, E.; Bergamini, M.; Lazzari, E.; Musacchio, A.; Mor, J.-R.; Pugliaro, E. Natural Background Levels of Potentially Toxic Elements in Groundwater from a Former Asbestos Mine in Serpentinite (Balangero, North Italy). *Water* **2021**, *13*, 735. <https://doi.org/10.3390/w13050735>

Academic Editor: Elisabetta Preziosi

Received: 30 January 2021

Accepted: 2 March 2021

Published: 8 March 2021

Publisher’s Note: MDPI stays neutral with regard to jurisdictional claims in published maps and institutional affiliations.



Copyright: © 2021 by the authors. Licensee MDPI, Basel, Switzerland. This article is an open access article distributed under the terms and conditions of the Creative Commons Attribution (CC BY) license (<https://creativecommons.org/licenses/by/4.0/>).

Keywords: trace metals; Lanzo Massif; ultramafic rocks; ophiolites; chromium; hexavalent chromium; nickel; neutral mine drainage

1. Introduction

Potentially toxic elements (PTEs), also known as trace or heavy metals [1], are always present in soils, being derived from the weathering of parent rocks that may contain them, and, depending on the hydrogeochemical context, may be found in groundwater too [2]. In the Anthropocene, high levels of PTEs have been introduced into the environment, affecting even ecosystems in remote areas [3]. In addition, acid rain, resulting from a change in atmospheric chemistry, has boosted soil and rock weathering and enhanced the solubility of metals in surface and groundwater [4], ultimately leading to increasing contents in water resources. As the human population heavily relies on groundwater for drinking water supply, threshold values (TVs) need to be established, corresponding to concentrations which should not be exceeded in order to protect human health and the environment [5,6].

Naturally high concentrations of PTEs in groundwater, exceeding the established TVs, represent a serious problem in many areas worldwide, affecting both hard rock [7,8] and sedimentary aquifers [9,10]. The anthropogenic contribution is less frequently observed,

as generally PTEs form cations or complexes, and are retained by the soil or the aquifer matrix. However, some PTEs with high ionic potential (e.g., As, Cr, V) can form oxyanions, especially in their high oxidation state. This is the case of hexavalent chromium (Cr VI), which has many industrial applications and originates well-identified contamination plumes in urban and industrial areas [11]. Great concern is therefore raised when Cr VI groundwater concentrations exceed the TV by reason of its high toxicity [12].

To protect the population from the negative impact of PTEs, the European Commission has promulgated the Groundwater Directive [13], as part of the more general Water Framework Directive [14]. This directive requires member states to set up monitoring networks and to define the groundwater quality status, based on defined TVs for potentially toxic substances, taking into account the natural background levels (NBLs). The TVs are valid nationwide and if, during monitoring activities, some groundwater samples exceed one or more TVs, the presence of anthropogenic contamination should be investigated [15].

The assessment of NBLs at the local scale can be performed using different procedures, that can be broadly classified into two approaches [16]. The pre-selection method requires the identification of groundwater monitoring stations (MSs) unaffected by anthropogenic pollution, based on a list of common contaminants (nitrates, ammonia and hydrocarbons). Once an adequate number of MSs are identified with “pristine” hydrochemical features, the NBLs of the dissolved substances are determined using statistical parameters such as the median concentration values or other selected percentiles. The second approach requires a statistical data treatment that recognises the presence of one or more data populations and, through component separation methods, extracts the “unaffected” MSs that are used to define the NBLs. An overview of the different procedures used to calculate NBLs [16], and of the common issues encountered in defining TVs and NBLs, is reported elsewhere [16,17].

The determination of NBLs is a difficult task in areas such as plain aquifers, generally affected by anthropogenic contamination, where uncontaminated MSs, but still representative of the natural groundwater hydrogeochemistry, are almost impossible to find [18]. Even more complicated is the determination of NBLs in hard rock aquifers, where the low and discontinuous permeability may give rise to groundwater characterised by different degrees of equilibration with the matrix, and consequently different mineralisation and PTE contents [19]. However, deriving NBLs for PTEs in mining environments represents a real challenge. Here, naturally high background concentrations may be present, which may be further increased by anthropogenic activities [20]. These, other than introducing exogenous substances or contaminants in groundwater, fuel up the natural water–rock interaction process. Indeed, rock excavation and crushing increase the specific surface area available for interactions with percolating waters, reduce the groundwater transit times and perturb the natural equilibrium by altering the pH-Eh conditions [21].

The main aim of this work is to illustrate the procedure followed to derive some PTE concentration values that can be reasonably adopted as NBLs in a former mining area. For legal reasons, the guidelines in force in Italy were followed [22], as far as possible. However, to account for the hydrogeological complexity of the area and to better exploit all the available monitoring data, some modifications of the procedure were necessary. In the paper, we discuss the derived NBLs based on the literature from similar hydrogeological settings, to support the conclusion on the natural origin of these high PTE concentrations.

2. Study Area

Located about 30 km NW of Turin, in the Piedmont region of North Italy (Figure 1), the former Balangero and Corio asbestos mine operated the extraction of chrysotile from the 1920s to the 1990s, becoming the largest asbestos mine in Western Europe. The mine is hosted in the serpentinised outer rim of the Lanzo Massif, one of the largest world outcrops of mantle peridotite, at the contact with the Sesia–Lanzo zone. The Lanzo Massif is a portion of subcontinental mantle that was exhumed to the seafloor during the opening of the Mesozoic Ligurian–Piedmontese oceanic basin [23,24]. The Sesia–Lanzo zone is a portion of continental crust from the African margin that, during the Alpine orogenesis,

was intensively folded and thrust, originating the present-day tectonic slices, hectometric to kilometric in size and E–W directed [25].

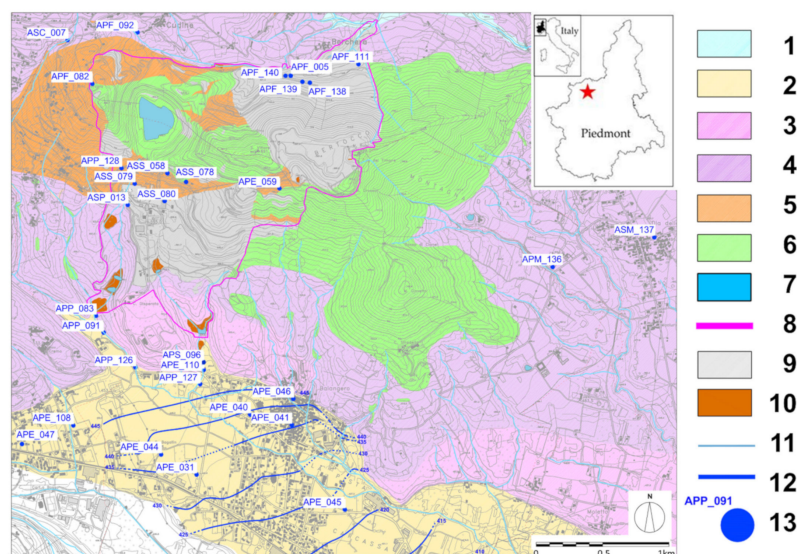


Figure 1. Location of the investigated area. 1 = recent alluvial deposits; 2 = alluvial deposits of the Balangero Plain (Middle–Upper Pleistocene); 3 = fluvioglacial deposits (Middle Pleistocene); 4 = fluvial deposits (Lower Pleistocene); 5 = Sesia-Lanzo zone; 6 = Lanzo Massif serpentinite; 7 = mine pit lake; 8 = remediation site; 9 = tailing piles; 10 = waste sludge; 11 = rivers; 12 = piezometric map of the phreatic aquifer from water table levels measured on Nov. 10–11, 2008 (m a.s.l.) [26]; 13 = monitoring station.

In the study area, the Lanzo Massif serpentinite is constituted by antigorite, diopside, chlorite, olivine and magnetite, with accessory Ni-Fe-Co alloys and sulphides [23,27,28]. The Sesia–Lanzo rocks are metabasites with glaucophane, epidote and garnet, associated with variable amounts of albite, chlorite, phengite, rutile, titanite, apatite, magnetite and sulphides (pyrite, chalcopyrite and covellite) [25]. Along the contact between the two units, a rodingite rim up to 6 m thick is present, originated by the metamorphism of original gabbro or basaltic intrusions. Rodingite is constituted by fine- to medium-grained diopside, irregularly alternated to garnet \pm chlorite, and hosts ore minerals (Fe-Cu-Zn-Pb-Ni-Co sulphides, Ni-Co-Fe arsenides and minor Fe-oxides) [27,28]. Finally, serpentinite is characterised by the presence of veins of different origin and composition, and variably associated metallic ores [29], among which are the stockwork chrysotile-rich veins (up to 15% in volume) that were exploited in the past [30]. In 1998, after the abandoning of the mining activities and following the increased evidence of human health effects among mine workers and the local population [31], the area was declared a “Contaminated Site of National Interest”, and its remediation is under the responsibility of the Italian Ministry of the Environment, Land and Sea.

The remediation site is located in a mountain area, extends for about 400 ha and includes the open mine pit, now occupied by a lake, the former industrial plant, now dismantled, and the mountain sides where mine tailings and waste sludge were dumped (Figure 1). Previous remediation activities included the stabilisation of the mine tailing piles, the removal of dumped waste sludge, and specific hydrogeological interventions to control runoff. These activities required the handling of large quantities of asbestos-rich materials, and were conducted following strict protocols to limit the potential health risk for workers and the surrounding inhabitants [32]. Since 2012, the remediation site was subject to an extensive characterisation of the presence of asbestos and of PTEs in soils, rivers and groundwater, to define the confinement and remediation strategies. During these monitoring activities, some PTE concentrations exceeding the established TVs were

detected in groundwater [15], in particular for Ni and Cr VI, triggering further investigation on their origin [22].

Hydrogeology

In the study area, four formations are potentially suitable to host groundwater. These are:

1. the crystalline rocks of the Sesia–Lanzo zone (henceforth indicated as SL);
2. the serpentinite of the Lanzo Massif (henceforth indicated as SERP);
3. the fluvial deposits, the glacial basal and ablation deposits of Middle Pleistocene, the fluvial deposits of Lower Pleistocene (grouped together as fluvioglacial deposits) and their colluvial–eluvial covers (henceforth indicated as FGD);
4. the alluvial deposits constituting the Balangero Plain (henceforth indicated as BPA).

The first two formations are constituted by massive rock bodies affected by fractures that can host groundwater mostly during the rainy seasons, in spring and in autumn. The fracture permeability, discontinuous by nature, does not allow considering these formations as “aquifers” according to the definition of ISPRA [22] (i.e., “one or more rock layers or other geological layers with a sufficiently high porosity and permeability to permit a significant groundwater flow or the extraction of significant amounts of groundwater” [15]). As such, the guidelines for the definition of NBLs would not be strictly applicable [22]. However, some wells, boreholes and springs located in these formations were also included. The water scarcity posed some difficulties in finding a sufficient number of MSs, located far from potential contamination sources related to the past mining activity. In addition, as the water-bearing fractures develop at the contact between the SL and the SERP formations, the attribution of each MS to one or to the other was based on borehole stratigraphy and on the geological expertise.

The fluvioglacial deposits and their colluvial–eluvial covers are located at the foothills of the mountain range. Although their origin is different, they share the same hydrogeological characteristics. Generally, these deposits have a limited thickness and low permeability, and therefore cannot be considered as “aquifers” [22]. No MSs are indicated on the geological map in this formation (Figure 1); however, the boreholes and wells located in the Balangero Plain, at the mountain foothills, are mostly developed in this formation, as indicated by their stratigraphy.

Finally, the Balangero alluvial deposits, located between the FGD and the Stura River, constitute the Lanzo valley floor. They originated from the dismantling of the SL and SERP rocks, mixed with the alluvial material transported by the river. They constitute a porous aquifer that can host phreatic groundwater. The piezometric map of this area shows a groundwater flow directed SSE from the mountain foothills towards the Stura River (Figure 1). Although located outside of the remediation site, this formation was included since it represents the natural outflow of the water recharged in the former mining site, it is the closest and the only aquifer of the area and it hosts villages and human settlements where monitoring stations can easily be found. Furthermore, the inhabitants of the area could be the target of the potential groundwater contamination leaking out of the remediation site.

3. Materials and Methods

3.1. The Italian Legislative Framework

The Italian TVs for the PTEs of concern are Cr = 50, Cr VI = 5, Co = 50, Ni = 20, Mn = 50, Fe = 200 and Zn = 3000 µg/L [15]. The guidelines for the evaluation of NBLs [22] indicate a complex multistep procedure that combines both the pre-selection and the component separation approaches. In the first phase of the procedure, based on the hydrogeological conceptual model, an adequate number of MSs should be identified. MSs should belong to the same hydrogeochemical context or facies, as defined by physico-chemical parameters and major ions’ concentrations. The MSs potentially affected by anthropogenic contamination, as indicated by the occurrence of nitrates, ammonia or

organic contaminants, should be disregarded. In the second phase, the investigation concentrates on the identification of temporal trends at those MSs with measurements performed at least 2 times per year over at least four years. This allows selecting, for each MS, the representative concentration values, generally corresponding to the median. These values are then examined to identify outliers, the presence of multiple populations and the statistical distribution of the MS dataset. In the third phase, the dataset size is assessed for its significance at the spatial (based on the number of MSs) and temporal scale (at least 8 half-yearly measurements for at least 80% of the MSs). Four cases could be present (A = significant size in space and time; B = significant size in space but not in time; C = significant size only in time; D = non-significant size), affecting the percentiles that can be used as NBLs and the confidence level attributed to this evaluation. For NBLs with low confidence levels, additional monitoring is required. More detailed information on the procedure is reported elsewhere [22,33]. In particular, the paper is organised in different sections, clearly referring to the different steps of the workflow, as reported by [33].

3.2. Sampling and Analytical Methods

Starting from 2012, several sampling campaigns were conducted on boreholes and wells from all the investigated formations, to assess the potential effects of the former mining activities on groundwater quality. However, the monitored parameters only included the main PTEs of concern (Cr, Cr VI, Co, Ni, Mn, Fe, Zn). These elements were determined at the Nuovi Servizi Ambientali S.r.l. laboratory (now Lifeanalytics Torino S.r.l.) by inductively coupled plasma optical emission spectroscopy (ICP-OES), with the exception of Cr VI, analysed by ultraviolet-visible spectroscopy (UV-VIS).

The complete hydrogeochemical characterisation requested by the guidelines for NBL assessment [22] was conducted in 2019 and included 30 MSs. Given the hydrogeological features of the study area, sampling was performed in spring (25 June to 4 July 2019), following a rainy period. Wells were purged prior to the collection of the water sample by pumping 3–4 times the well volume with a low-flow pump, until the stabilisation of the physico-chemical parameters. In some cases, where purging was not possible, the sample collection was performed with a bailer. Temperature, redox potential, electrical conductivity (E.C.), pH and dissolved oxygen were measured in the field with the HACH HQ40D multiparameter probe and a flow chamber to avoid any contact with the atmosphere. The field redox potential was corrected to report the values relative to the standard hydrogen electrode. Alkalinity was also measured in the field with the HACH Digital Titrator and standardized titration cartridges. Water samples for anion analyses were collected in high-density polyethylene (HDPE) pre-washed containers. The sample aliquot for cation and trace element analyses was filtered in the field to 0.45 µm and acidified with ultrapure chloridric acid. Samples for hydrocarbon analyses were collected in dark glass containers.

The parameters determined in the laboratory included the main cations and anions (Ca^{2+} , Mg^{2+} , Na^+ , K^+ , NH_4^+ , SO_4^{2-} , Cl^- , HCO_3^- , NO_3^-); the elemental concentrations of Si, Al and PTEs (Cr, Cr VI, Co, Ni, Mn, Fe, Zn); and the total hydrocarbon content (light and heavy fractions). All the analyses were performed by the Nuovi Servizi Ambientali S.r.l. (now Lifeanalytics Torino S.r.l.) laboratory, following approved standard analytical methods [34]. In particular, PTEs were determined by the same techniques adopted during previous investigations. The results are reported in Table S1 (field parameters, major ions and ionic balance) and Table S2 (minor and trace elements), both in the Supplementary Materials.

3.3. Data Validation and Selection

The analytical quality check was performed by calculating the charge balance error using major ions (Ca^{2+} , Mg^{2+} , Na^+ , K^+ , SO_4^{2-} , Cl^- , HCO_3^- , NO_3^-), and considering as acceptable a value (Err. %) lower than 10% (Table S1) [6]. All the samples have an acceptable ionic balance error except APF140. This sample has a very low mineralisation (calculated Total Dissolved Solids = 71 mg/L) and a low Eh (191 mV), allowing high Fe

contents in solution ($\text{Fe} = 1583 \mu\text{g/L}$). If this is accounted for (as Fe^{2+}), the ionic balance fits within the limits.

Among major cations, Na^+ and K^+ sometimes showed contents below the limit of detection (LOD) of 0.5 mg/L. As these were necessary to define the hydrochemical facies, the values $< \text{LOD}$ were substituted with a concentration value equal to half the LOD. Concerning NH_4^+ , only five samples had detectable concentrations of this parameter ($\text{LOD} = 0.026 \text{ mg/L}$). Si is ubiquitous ($\text{LOD} = 1 \text{ mg/L}$), as only six samples are below the LOD; on the other hand, Al ($\text{LOD} = 0.001 \text{ mg/L}$) could be analysed in eight samples only. By contrast, the PTEs of concern in the NBL evaluation (Cr, Cr VI, Co, Ni, Mn, Fe, Zn) commonly show concentrations $< \text{LOD}$ ($\text{LOD} = 1 \mu\text{g/L}$, for Cr VI $\text{LOD} = 3 \mu\text{g/L}$), as observed in a consistent and variable number of samples (Tables S2 and S3 in the Supplementary Materials). A concentration of half the LOD was substituted for all concentrations $< \text{LOD}$, as this choice has little influence on the upper tail of the distribution curve (i.e., percentiles $\geq 90\text{p}$) [22]. The section dedicated to NBL calculations discusses in detail this choice and its consequences.

4. Results

4.1. Hydrochemical Facies

The graphical representation of hydrochemical data was performed to describe the water quality, compare the samples to identify similarities and differences and suggest the specific processes affecting the composition during its evolution (i.e., water–rock interaction processes). As this study deals with PTEs, water samples were first classified based on Eh and pH (Figure 2) [35].

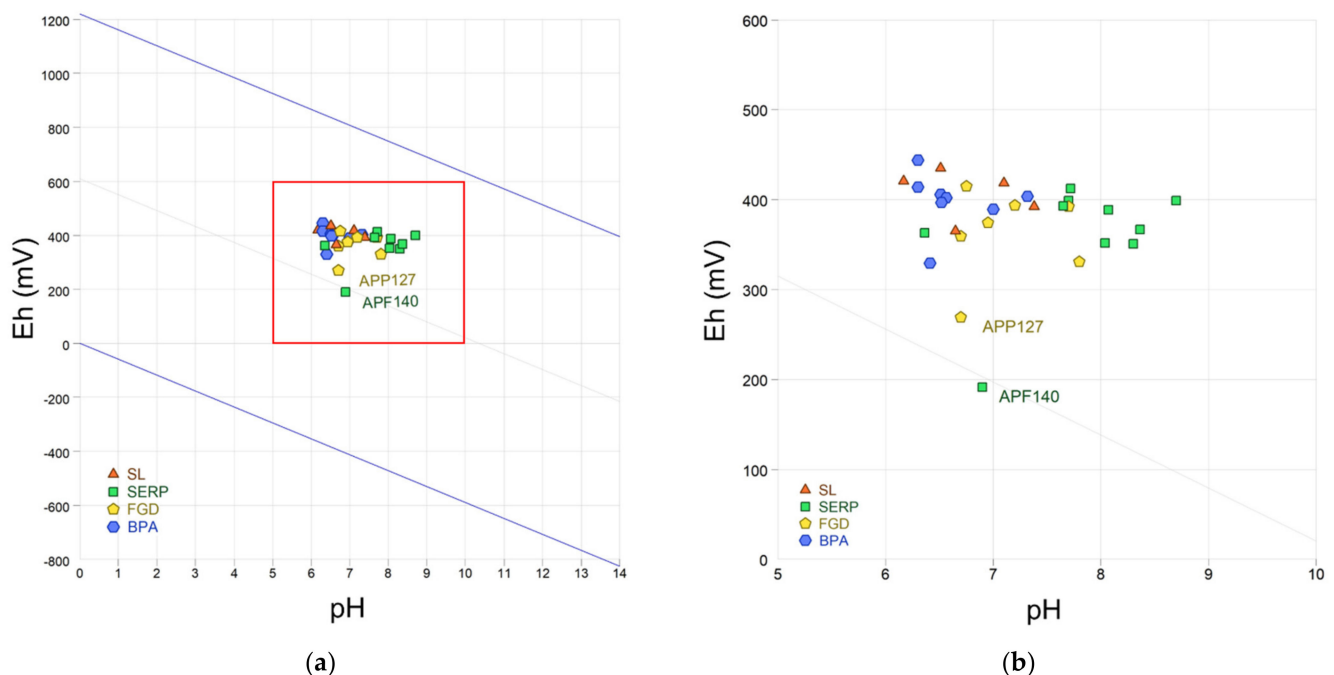


Figure 2. Eh–pH diagrams: (a) full plot, where the blue lines indicate the stability field of liquid water; (b) an enlargement of the portion indicated in red.

Samples are characterised by a circumneutral pH (6.17 to 8.70) in line with the natural range of most natural groundwater [36] unaffected by anthropogenic contamination or acid mine drainage [21]. Eh values (mV) range between 191 and 444, corresponding to dissolved oxygen contents from 1.90 to 10.0 mg/L. Most of the samples can be classified as oxidic, except for APP127 (FGD) and APF140 (SERP) that are closer to the limit of reducing waters (Figure 2).

The hydrochemical facies was defined using a Piper diagram [37] (Figure 3), where the major anions and cations are reported in meq/L (%).

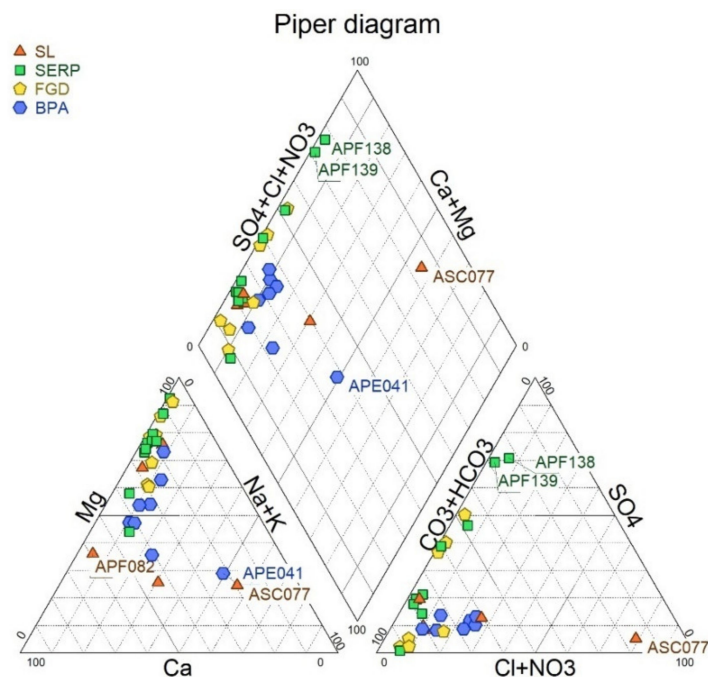


Figure 3. Piper diagram.

Concerning cations, most of the samples have a Mg facies, this element being very abundant in rocks from the SERP and SL formations. Only sample APF082 (SL), collected close to a rodingite vein, which is rich in Ca-bearing silicates [28], has a Ca facies. All the other samples fall in the field of non-dominant cations. Sample APE041 (BPA), close to the field of dominant Na and K, shows high concentrations of K^+ , even greater than Na^+ , which is uncommon in natural waters. This high K^+ concentration could be due to anthropogenic contamination as the sample belongs to a well located in the Balangero village. Finally, sample ASC077 (SL), a spring collected following some intense precipitation events, has a Na-K facies. As for the anions, most of the samples are of HCO_3^- facies, with a tendency towards the SO_4 facies with increasing mineralisation, as indicated by the significant correlation between E.C. and SO_4^{2-} ($N = 30$; $R^2 = 0.67$; $p < 0.01$). Samples APF138 and APF139 (SERP) are, instead, of SO_4 facies. These were collected at the foothills of the Fandaglia mine waste dump, where rock debris were accumulated. The presence of sulphides in the SERP formation is well known [38], and sulphates could derive from the oxidation of these minerals, as is commonly observed in mining areas [21]. Finally, ASC077 (SL) is the only sample of Cl facies.

In conclusion, the dominant hydrochemical facies is $Mg-HCO_3$, and no systematic changes in hydrochemistry are observed between samples from different formations. Waters tend to evolve towards a sulphate-rich facies, turning to $Mg-HCO_3$ (SO_4) facies. Two samples from the SERP formation are of $Mg-SO_4$ facies and one from the SL formation is of Na-Cl facies.

These observations are confirmed by the Stiff diagrams [39], where samples are represented in the order of increasing mineralisation and with different colours according to their formation (Figure S1 in the Supplementary Materials). The shape of the polygons is very similar, regardless of the formation, and the dominant facies is $Mg-HCO_3$. The only exceptions are those already evidenced by the Piper diagram, i.e., the two low-mineralised samples ASC077 (Na-Cl) and APF082 ($Ca-HCO_3$), both of the SL formation, the medium-mineralised sample APE041 (PBA) for its K^+ content and the two highly mineralised samples APF138 and APF139 (SERP) for their SO_4^{2-} content.

Based on these results, the collected samples appear to belong to the same hydro-geochemical context characterised by silicate Mg-rich rocks and sediments, and their weathering products. The rocks are locally affected by ore deposits (e.g., rodingite and metal sulphides both in veins or disseminated in the matrix [28]), whose weathering may slightly change the hydrochemical facies. Consequently, the four formations host groundwater with very similar characteristics. The only exception is sample ASC077 with a low mineralisation and a Na-Cl facies. This sample was collected close to a road, and the Na:Cl molar ratio of 1:1 suggests that these ions may derive from de-icing salt. Nevertheless, the PTE concentrations of this sample do not differ from the others and its inclusion in the dataset does not modify its characteristics.

4.2. Pre-Selection

This step aims at eliminating from the dataset the MSs with evidence of anthropogenic contamination based on the presence of some indicators (i.e., nitrates, ammonia, hydrocarbons).

For nitrates and ammonia, only samples below the concentration of 37.5 mg/L and 0.375 mg/L, respectively, corresponding to 75% of the TV allowed in drinking water, were retained in the dataset [22]. Indeed, since the BPA hosts villages and housing, a lower threshold (e.g., 10 mg/L for NO_3^-) would have required the exclusion of numerous MSs from this formation. Only one MS, APE040 (BPA), exceeded the threshold level for nitrates and was therefore eliminated from the dataset. No sample exceeds the limit for ammonia. Concerning hydrocarbons, the regulations only indicate a TV of 350 $\mu\text{g/L}$ for total hydrocarbons expressed as n-hexane. All the results are below this limit. Low concentrations (1–2 $\mu\text{g/L}$, expressed as n-hexane) of light hydrocarbons (C5–C10) are present in a few samples from all the formations with the exception of SL. However, based on the literature, it is supposed that they could be of natural abiotic origin [40].

Having demonstrated that the MSs belong to the same hydrogeochemical context, the PTE dataset to be used for the evaluation of the NBLs was integrated with the results of previous campaigns, in order to have a sufficient amount of data for statistical treatment. All the available PTE measurements are reported in Table S3 (Supplementary Materials), where the values marked in bold exceed the TVs for groundwater quality [15].

5. Data Treatment

5.1. Trend Analysis

The available dataset is unsuitable to evaluate the presence of temporal trends, as no MS has a series of 8 measurements with a regular frequency extending for at least 2 years (Table S3), as requested by the guidelines [22]. Nevertheless, the trend analysis was performed for the two MSs, APP126 (FGD) and APE031 (BPA), with a sufficient number of measurements (11 and 10, respectively, although with some missing values). The procedure first involves a check for the presence of outliers, followed by the application of the Mann–Kendall test, that does not assume a normal distribution and permits missing data [41,42]. However, the test requires a regular sampling frequency. Since in our case the number of samplings varies between zero and three per year, the year was selected as a time unit and, for the years where multiple sampling were present, a random selection was performed [43].

In the case of APP126 (FGD), the sampling dates randomly selected were 24 July 2015, 3 February 2016, 20 April 2017, 12 January 2018 and 25 June 2019, and no significant trends for Cr, Cr VI, Ni and Mn were detected (Table S4 in Supplementary Materials).

Concerning APE031 (BPA), this MS was sampled first in 2012, then was not monitored for two years, and then was sampled regularly starting from 2015 (Table S3). If the trend analysis is conducted for the period 2015–2019 and using the randomly selected samplings of 24 July 2015, 14 December 2016, 20 April 2017, 12 January 2018 and 25 June 2019, the trend hypothesis is rejected for Cr, Mn and Ni. However, if 2012 is also included in the analysis, and the missing measurements of 2013 and 2014 are estimated by linear interpolation, a significant trend for Ni and for Mn is detected (Table S4). Using Sen's slope

estimator [44], a decreasing trend for Ni of $-7.87 \mu\text{g/L}$ per year and an increasing trend for Mn of $+0.27 \mu\text{g/L}$ per year are identified. In conclusion, for both stations, the trend analysis is not sufficiently sound to detect changes in time, and given the overall agreement of PTE concentrations with the other stations of the dataset, they will not be eliminated for subsequent treatment.

5.2. Spatial Analysis

The synthesis table with the PTEs' representative values for each MS is presented as Table 1. For the MSs only sampled once, the measured PTE concentrations are assumed as representative. For the MSs sampled more than once, the median concentration value of each element is considered as representative. In addition, Table 1 reports the total number of MSs, the number of values < LOD and the percentage of non-detected values (%ND). In this regard, Co and Cr VI, with 97% and 79% of ND data, respectively, are the more problematic.

Table 1. Synthesis table reporting the potentially toxic element (PTE) representative values for each monitoring station (MS). Unit: SL = Sesia-Lanzo; SERP = Serpentinite; FGD = Fluvio-glacial Deposits; BPA = Balangero Plain Aquifer. Values in italic correspond to those < limit of detection (LOD). Values in bold exceed the threshold values (TVs) for water quality [15]. % ND = percentage of non-detected values.

Monitoring Station	Unit	Cr $\mu\text{g/L}$	Cr VI $\mu\text{g/L}$	Co $\mu\text{g/L}$	Ni $\mu\text{g/L}$	Mn $\mu\text{g/L}$	Fe $\mu\text{g/L}$	Zn $\mu\text{g/L}$
APE031	BPA	1.0	1.5	0.5	71.3	1.3	7.2	38.4
APS096	FGD	4.8	1.5	0.5	23.9	5.8	1.6	0.5
APP126	FGD	17.8	14.1	0.5	1.7	0.5	0.5	0.5
APF082	SL	11.0	3.3	0.5	20.4	4.4	329.9	15.5
APP128	SL	4.7	3.6	0.5	14.4	8.1	0.5	0.5
APP127	FGD	0.5	1.5	2.9	8.9	1571.5	966.0	0.5
APE059	SERP	4.5	1.5	0.5	26.6	17.7	3.4	0.5
ASS078	SERP	6.7	1.5	0.5	8.7	2.3	4.3	0.5
ASS058	SERP	1.4	1.5	0.5	2.5	0.5	8.6	0.5
ASS080	SERP	2.7	1.5	0.5	8.5	1.0	3.5	0.5
APE047	BPA	1.6	1.5	0.5	56.6	0.5	0.5	0.5
APE108	BPA	2.4	1.5	0.5	32.3	2.5	0.5	46.2
APE044	BPA	0.5	1.5	0.5	37.8	22.0	7.9	213.5
APE045	BPA	0.5	1.5	0.5	37.5	2.7	0.5	33.7
APE041	BPA	3.9	1.5	0.5	6.1	0.5	0.5	57.0
APE046	BPA	5.4	1.5	0.5	2.5	0.5	0.5	27.0
APP091	FGD	1.7	1.5	0.5	5.6	0.5	1.1	21.4
APE110	FGD	3.6	1.5	0.5	17.7	0.5	0.5	11.4
APF092	SL	0.5	1.5	0.5	1.4	6.8	30.0	0.9
ASP013	SERP	8.5	3.8	0.5	34.1	0.5	0.5	0.5
APP083	FGD	6.8	6.7	0.5	0.9	0.5	3.4	0.5
ASS79	SL	4.8	1.5	0.5	16.0	4.0	0.5	0.5
APF111	SERP	3.9	1.5	0.5	12.1	0.5	0.5	0.5
APF139	SERP	0.5	1.5	0.5	8.9	2.1	19.5	0.5
APF005	SERP	41.0	38.1	0.5	0.5	0.5	1.5	0.5
APF138	SERP	1.9	1.5	0.5	1.6	6.8	38.9	0.5
APF140	SERP	0.5	1.5	0.5	0.5	125.0	1583.0	0.5
ASM137	FGD	0.5	1.5	0.5	15.8	0.5	0.5	0.5
ASC077	SL	0.5	1.5	0.5	0.5	5.3	0.5	3.6
MS		29	29	29	29	29	29	29
< LOD		8	23	28	3	12	12	18
% ND		28	79	97	10	41	41	62

Graphical methods such as boxplots and normal quantile–quantile (Q–Q) plots were used to evaluate potential outliers among the MSs. In the boxplots, the MSs with values exceeding 1.5 times the difference between 25p and 75p were considered as potential

outliers. In the normal Q–Q plots, a line represents the normal distribution, and the potential outliers are those plotting far from it. The results are discussed for each element, with the exception of Co that is detected in only one station, and the relative plots are reported in the Supplementary Materials (Figure S2).

5.2.1. Total and Hexavalent Chromium

The two parameters are jointly discussed, since numerous MSs have ND values of Cr VI, and since they are significantly correlated ($N = 29$; $R^2 = 0.92$; $p < 0.01$). Two MSs, APF005 (SERP) and APP126 (FGD), were identified as potential outliers in the boxplots. These two MSs have medium–low mineralisation and belong to the dominant Mg-HCO₃ facies. In the Cr VI boxplot, due to the large number of ND values, all the detected values are identified as outliers. Normal Q–Q plots indicate that the two parameters are not normally distributed, but do align in the plot, suggesting that the distribution can be normalised. For these reasons, the two potential outlier MSs do not seem to show any particular reason to be excluded from the dataset for calculation of NBLs.

5.2.2. Nickel

The Ni boxplot evidences only one MS as a potential outlier, APE031, that shows the highest representative value. The normal Q–Q plot suggests that this element could have a normal distribution but also indicates an additional MS as potential outlier, APE047. Both MSs belong to the BPA formation, have a Mg-HCO₃ facies and intermediate mineralisation and do not show any peculiarity supporting their elimination from the dataset for calculating the Ni NBL.

5.2.3. Manganese

Four MSs showing representative concentrations greater than 10 µg/L are identified in the boxplot as potential outliers. These are, in decreasing concentration order:

- APP127 (FGD), with a Mg-HCO₃(SO₄) facies. This MS is the only one where Co was detected, and has the second highest Fe concentration. These elements could be present in solution because of the relatively low redox potential. This station has been repeatedly monitored (Table S3), and the well stratigraphy has identified Mn oxide deposits;
- APF140 (SERP), an MS with low mineralisation and Mg-HCO₃ facies. This MS shows the highest Fe concentration and is the only one with a reducing Eh (Figure 2);
- APE044 (BPA), with medium mineralisation and Mg-HCO₃ facies. This MS has elevated Zn concentrations, but average Ni concentrations;
- APE059 (SERP), with medium–low mineralisation and Mg-HCO₃ facies.

The normal Q–Q plot indicates that the data strongly deviate from a normal distribution. The two MSs plotted far from the normality line are the two first stations.

For the reasons discussed above, none of these stations can be reasonably eliminated from the dataset for the calculation of NBLs. Even those stations with low redox potential, which display the higher Mn concentrations, are likely reducing for natural reasons since no other organic indicator of contamination, such as hydrocarbons, was detected in these samples.

5.2.4. Iron

The Fe plots are very similar to those of Mn. Five MSs are indicated as potential outliers, in decreasing concentration order:

- APF140 (SERP) and APP127 (FGD), showing high Fe concentrations because of their low redox potential;
- APF082 (SL), with a low mineralisation and a Ca-HCO₃ facies. The MS is located close to a rodingite vein, constituted by Ca-rich silicates hosting metallic ores [28];

- APF138 (SERP), with high mineralisation and Mg-SO₄ facies. As previously discussed, this MS is located at the foothills of the Fandaglia mine waste dump and its Fe content could derive from oxidation of sulphides disseminated in serpentinite;
- APF092 (SL), with very low mineralisation and Mg(Ca)-HCO₃ facies. This MS is very similar in hydrochemistry to APF082, and could contain Fe for the same reason.

Therefore, also in the case of Fe, there are no reasons to eliminate any MS from the dataset for the determination of NBLs, as all the possible outliers could be derived from natural water–rock interaction processes.

5.2.5. Zinc

The Zn boxplot evidences two stations as potential outliers:

- APE044 (BPA), an MS already shown to have a high Mn concentration;
- APE041 (BPA), an MS with K⁺ concentrations higher than Na⁺, an uncommon feature in natural waters. Being located in the Balangero village, this well could reflect some anthropogenic contamination.

While the latter station could reasonably be eliminated from the dataset, this would have few consequences since the Zn concentration is not very high and the other PTEs are not anomalous as well. The normal Q–Q plot confirms the choice not to delete this MS, as the data do not show a normal distribution but are well aligned. Based on this plot, only APE044 would be a potential outlier.

5.3. Statistical Distribution

The statistical distribution was evaluated in the dataset of the representative PTE values for each MS (Table 1). The descriptive statistics are reported in Table 2.

Table 2. Descriptive statistics of the representative PTE values (in µg/L) for each MS.

Including ND Data		Cr	Cr VI	Co	Ni	Mn	Fe	Zn
N	Valid	29	29	29	29	29	29	29
	Missing	0	0	0	0	0	0	0
	Mean	4.965	3.588	0.583	16.376	61.898	104.007	16.466
	Median	2.700	1.500	0.500	8.900	2.100	1.500	0.500
	Mode	0.5	1.5	0.5	0.5	0.5	0.5	0.5
	Std. Deviation	7.9155	7.0997	0.4457	17.7297	291.25	340.02	41.0952
	Skewness	3.730	4.511	5.385	1.554	5.333	3.768	4.245
	Kurtosis	16.028	21.586	29.000	2.382	28.596	14.339	20.118
	Minimum	0.5	1.5	0.5	0.5	0.5	0.5	0.5
	Maximum	41.0	38.1	2.9	71.3	1571.5	1583.0	213.5
Percentiles	25	0.500	1.500	0.500	2.100	0.500	0.500	0.500
	50	2.700	1.500	0.500	8.900	2.100	1.500	0.500
	75	5.100	1.500	0.500	25.250	6.300	8.225	18.425
	90	11.000	6.650	0.500	37.800	21.950	329.90	46.200
	95	29.400	26.100	1.700	63.925	848.25	1274.0	135.25

All the parameters have a non-normal distribution, as indicated by the non-corresponding mean and median values, and by the positive skewness that suggests a tail extending towards high values. The mode for all parameters corresponds to the value adopted for the data < LOD (0.5 µg/L for all PTEs except Cr VI = 1.5 µg/L). Frequency histograms (Figure S3 in the Supplementary Materials) show the same pattern, with a mode corresponding to the lowest values. This suggests the absence of a normal distribution but the presence of a single population with a distribution that can be normalised.

Although the presence of numerous MSs with ND data (Table 1, Figure S3) likely affects the distribution, if these are eliminated, the distribution still shows a strong positive skewness (Table 3); however, some elements (Cr, Cr VI, Fe, Zn) display multiple modes, while Ni and Mn remain unimodal.

Table 3. Descriptive statistics of the representative PTE values (in µg/L) for each MS, excluding ND.

Excluding ND		Cr	Cr VI	Co	Ni	Mn	Fe	Zn
N	Valid	21	6	1	26	17	16	11
	Missing	8	23	28	3	12	13	18
	Mean	6666	11.592	2.900	18.208	105.238	188.106	42.591
	Median	4500	5.225	2.900	13.225	5.300	7.525	27.000
	Mode	3.9 ^a	3.3 ^a	2.9	2.5	6.8	1.1 ^a	0.8 ^a
	Std. Deviation	8.7581	13.6142		17.8417	378.98	446.08	59.3218
	Skewness	3.373	2.017		1.480	4.083	2.672	2.810
	Kurtosis	12.675	4.079		2.138	16.755	6.774	8.570
	Minimum	1.0	3.3	2.9	0.8	1.0	1.1	0.8
	Maximum	41.0	38.1	2.9	71.3	1571.5	1583.0	213.5
Percentiles	25	2.150	3.525	2.900	4.788	2.350	3.362	11.400
	50	4.500	5.225	2.900	13.225	5.300	7.525	27.000
	75	6.725	20.100	2.900	28.013	12.875	36.675	46.200
	90	16.440	38.100	2.900	43.425	414.30	1151.1	182.20
	95	38.680	38.100	2.900	66.137	1571.5	1583.0	213.50

a. Multiple modes exist. The smallest value is shown.

To test if the MS representative values have normal or lognormal distribution, the Shapiro–Wilk test was applied to the data and to their logarithm [45]. The test rejects the normal distribution hypothesis in all cases, except for Ni that shows an almost significant lognormal distribution. However, if we exclude the MSs with ND values, the Shapiro–Wilk test on log data accepts the hypothesis for Cr, Cr VI, Ni and Zn, indicating that their distribution is lognormal and therefore can be normalised.

The non-normal distribution of Fe and Mn, even eliminating the MSs with ND values, is likely related to the presence of two MSs with very high contents (APP127 and APF140), because of their low redox potential. If these are eliminated from the dataset (Table 1), Cr and Ni show a lognormal distribution; if, in addition, the ND values are omitted, all the PTEs display a lognormal distribution. These results are summarised in Table S5 (Supplementary Materials).

In conclusion, results indicate that for Cr, Cr VI, Ni and Zn, the MSs belong to one single population that can be treated to obtain the NBLs. For Fe and Mn, the exclusion of the MSs APP127 and APF140 because of their low redox potential should be further evaluated, based on all the available measurements.

5.4. Assessment of the Dataset

Since the different MSs constitute a statistically representative homogenous population, belonging to the same hydrogeochemical context, all the measurements available from previous campaigns can be used to evaluate the NBLs of total Cr, Cr VI, Co, Ni, Mn, Fe and Zn (Table S3 in the Supplementary Materials), so as to deal with sufficiently large amounts of data. Unfortunately, not all the MSs have been analysed more than once and for all the PTEs, leading to variable numbers of measurements, from 74 for Mn to 39 for Fe and Zn (Table 4). However, both the number of MSs sampled at least once (29) and the total number of PTE measurements (39–74) exceed the minimum number required for a significant spatial analysis. On the other hand, as already detailed, the measurements do not show an adequate temporal dimension (i.e., there are no MSs with at least 8 measurements with a regular frequency over at least two years, see Section 5.1). Therefore, the temporal dimension of the dataset is not significant. Accordingly, this dataset is classified as type B [22].

Table 4. Descriptive statistics of the total number of PTE measurements (in µg/L) (Table S3), including ND.

Including ND		Cr	Cr VI	Co	Ni	Mn	Fe	Zn
N	Valid	71	67	71	71	74	39	39
	Missing	3	7	3	3	0	35	35
	Mean	4.965	6.979	5.473	0.654	21.332	183.1	87.249
	Median	2.700	3.1	1.5	0.5	9.1	1.1	1.7
	Mode	0.5	0.5	1.5	0.5	0.5	0.5	0.5
	Std. Deviation	7.9155	9.51	7.909	0.915	25.790	844.760	305.937
	Skewness	3.730	2.139	2.591	5.959	1.519	5.401	4.042
	Kurtosis	16.028	4.584	7.392	35.02	1.764	30.038	16.787
	Minimum	0.5	0.5	1.5	0.5	0.5	0.5	0.5
	Maximum	41.0	41.4	38.1	6.6	109	5554	1583
Percentiles	25	0.5	1.5	0.5	1.8	0.5	0.5	0.5
	50	3.1	1.5	0.5	9.1	1.1	1.7	0.5
	75	7.4	6.5	0.5	34	6.05	8	11.4
	90	19.6	15.0	0.5	64.06	46.74	58.40	57.00
	95	31.1	21.4	0.5	78.78	1568.75	966	120

The descriptive statistics of the dataset are reported in Table 4.

Concerning Co, the statistics are not relevant as this element shows only two measurements > LOD, both from the same MS. All the parameters have a non-normal distribution, as indicated by the non-corresponding mean and median values. The positive skewness suggests a tail extending towards high values. As for the case of the MS dataset, the mode for all parameters corresponds to the value adopted for the results < LOD (0.5 µg/L for all PTEs except Cr VI = 1.5 µg/L).

The descriptive statistics of the dataset excluding the ND still show a positive skewness but also the presence of multiple modes (Table 5).

Table 5. Descriptive statistics of the total number of PTE measurements (in µg/L) (Table S3), excluding ND.

Excluding ND		Cr	Cr VI	Co	Ni	Mn	Fe	Zn
N	Valid	53	21	2	63	38	21	13
	Missing	21	53	72	11	36	53	61
	Mean	6666	9.179	14.176	5.95	23.978	356.089	161.605
	Median	4500	5.4	12.8	5.95	12.1	5.55	6.4
	Mode	3.9 ^a	1.6	12.8 ^a	5.3 ^a	1.2 ^a	1.8	1.6 ^a
	Std. Deviation	8.7581	10.1134	9.5163	0.9192	26.2264	1159.6447	406.5181
	Skewness	3.373	1.824	1.526		1.39	3.759	2.829
	Kurtosis	12.675	3.085	2.253		1.355	14.046	7.774
	Minimum	1.0	1	3.8	5.3	1.1	1	1.6
	Maximum	41.0	41.4	38.1	6.6	109	5554	1583
Percentiles	25	1.85	6.65	5.3	3.4	2.475	2.65	7.5
	50	5.4	12.8	5.95	12.1	5.55	6.4	33.7
	75	14.75	18.1	6.6	34.3	21.1	29.85	66.65
	90	21.68	34.88	6.6	68.86	1567.1	900.6	232.2
	95	39.2	38.1	6.6	82.26	4392.15	1521.3	307

^a. Multiple modes exist. The smallest value is shown.

Frequency histograms (Figure S4 in the Supplementary Materials) show the same pattern, with a mode corresponding to the lowest values and a marked positive skewness. The presence of a second mode is particularly evident for total Cr. The measurements >10 µg/L belong to the MSs APE031 (BPA), APP126 (FGD), APF082 (SL) and APF005 (SERP), all attributed to the same hydrogeochemical context.

Despite the presence of multiple modes, the D'Agostino (for a number of available measurements ≥50) or Shapiro-Wilk (for a lower number of measurements) statistical tests were applied to the data or to their logarithm to check for the presence of a normal

distribution [45,46]. The results are shown in Table S6 (Supplementary Materials). The tests on all the PTE measurements indicate that they do not have a normal distribution, but Cr and Ni have a lognormal distribution. If ND values are excluded, all PTEs have a lognormal distribution except Fe and Mn. The non-normal distribution of Fe and Mn, even eliminating the ND values, is likely related to high concentrations recorded in two MSs (APP127 and APF140), because of their low redox potential. If the measurements from these two MSs are eliminated from the dataset, Cr and Ni show a lognormal distribution; if, in addition, the ND values are omitted, all the PTEs display a lognormal distribution, with the exception of Fe. This is due to the presence of one measurement (Fe = 639 µg/L, dated 17/04/2012, Table S3) from the MS APF082 (SL). This MS has a Ca-HCO₃ facies and is located close to a rodingite vein, enriched in metal ores. The MS was indicated as a potential outlier (see Section 5.2.4), but was not excluded because, using the median value to represent the MS, Fe displayed a lognormal distribution (Table S5 in the Supplementary Materials). Therefore, as a first approximation, we will keep this measurement in the dataset for further elaboration.

5.5. Evaluation of NBLs

As already indicated, the dataset has a significant spatial dimension, but its temporal dimension is not adequate, allowing us to classify it as B type [22]. This does not change the procedure to calculate the NBLs with respect to a dataset of the A type (significant for both spatial and temporal dimension), but only the confidence level attributed to the evaluation.

According to the guidelines [22], the evaluation should be based on the representative PTE values for each MS, corresponding to the median value for those MSs sampled more than once, and to the single measurement for the MSs measured only once (Table 1). Indeed, it was previously demonstrated that, for each PTE except for Fe and Mn, the data distribution can be normalised if ND values are excluded. However, ND values are numerous, especially for Cr VI, Co and Zn. The percentiles (90p and 95p) that could be used as NBLs are reported in Table 6, compared to the maximum concentrations recorded. For some PTEs with a low number of MSs showing detectable concentrations (e.g., Cr VI or Co), these percentiles correspond to the maximum measured concentration. For this reason, the guidelines suggest to use a lower percentile for MSs with a low number of detected values (N). In addition, if the two MSs with a low redox potential, APP127 (FGD) and APF140 (SERP), are eliminated from the dataset, Fe and Mn can be normalised too, but this also reduces N. The comparison is shown in Table 6. No differences are observed with respect to the previously calculated percentiles except for those of Fe and Mn that are noticeably lower. However, since APP127 (FGD) is the only station with detectable Co concentrations, the percentiles for this element cannot be determined.

Table 6. PTE percentiles calculated using the representative PTE values (in µg/L) for each MS (Table 1). In bold, the values exceeding the TVs for water quality [15].

	Data from Table 1 Without ND				Excluding the MSs APP127 and APF140			
	N	Max	95p	90p	N	Max	95p	90p
Cr	21	41	38.7	16.44	21	41	38.7	16.44
Cr VI	6	38.1	38.1	38.1	6	38.1	38.1	38.1
Co	1	2.9	2.9	2.9	0	NA	NA	NA
Ni	26	71.3	66.1	43.42	25	71.3	66.9	45.3
Mn	17	1571.5	1571.5	414.3	15	22.0	21.95	19.4
Fe	16	1583	1583	1151.1	14	329.9	329.9	184.4
Zn	11	213.5	213.5	182.2	11	213.5	213.5	182.2

Moreover, it must be noted that, when using the median value as representative for the MSs, half of the values are eliminated from the calculation of the percentiles, and particularly the higher ones. While this is necessary and justified when the aim is to eliminate from the dataset those MSs potentially affected by anthropogenic contamination,

it is less acceptable when the aim is to define the highest concentrations that can be reached in a natural context, unaffected by anthropogenic contamination, such as that of the study area. For comparison, Table 7 reports the percentiles calculated based on all the available measurements (Table S3).

Table 7. PTE percentiles calculated using the total number of PTE measurements (in $\mu\text{g/L}$) (Table S3). In bold, the values exceeding the TVs for water quality [15].

	Data from Table S3 Without ND				Excluding Data from APP127 and APF140			
	N	Max	95p	90p	N	Max	95p	90p
Cr	52	41.4	39.2	21.68	52	41.4	39.3	21.86
Cr VI	21	38.1	38.1	34.88	21	38.1	38.1	34.88
Co	2	6.6	6.6	6.6	0	NA	NA	NA
Ni	63	109	82.26	68.86	59	109	84.0	71.3
Mn	38	5554	4392	1567	32	92.1	71.36	27.22
Fe	21	1583	1521	900.6	19	639	630	58.4
Zn	13	307	307	232.2	13	307	307	232.2

Comparing the results that exclude the measurements from the two MSs with low redox potential, the percentiles calculated for Cr and Cr VI are little affected, whereas changes are observed in the percentiles for Ni, Zn and especially for Fe and Mn. In addition, in this case, the 95p values for Cr VI, Ni, Mn and Fe largely exceed the TVs for water quality [15]. The rationale to select one or another value as an NBL will therefore be evaluated based on the literature from similar hydrogeological settings.

6. Discussion

The study area is characterised by the presence of ferromagnesian rocks (ultramafic serpentinite, stratified rodingite or in veins, metabasites of the SL complex), and by sediments derived from their erosion. In addition, the presence of metal ores has been assessed (oxides, sulphides and Fe-Ni-Co alloys together with other metals). In this geochemical context, the considered PTEs are mostly present in their reduced form (oxidation state +2 for Fe, Mn, Co, Ni and Zn, +3 for Cr). The weathering of primary minerals can mobilise and solubilise these elements, at different concentrations and ratios, depending on the environmental geochemical conditions. At circumneutral pH, Fe and Mn are only soluble in reducing environments, whereas in oxidising environments, they precipitate, forming oxy-hydroxides. The high specific surface of these minerals may favour the co-precipitation of other elements, such as Co, Cr III and Zn, whose concentration in oxic waters is generally low. By contrast, Ni and Cr VI are more mobile. In particular, the latter can form oxyanions that are poorly retained by the aquifer matrix [47].

In the following discussion, the 95p values evaluated for the study area are compared with the concentrations reported in other regional, national and international studies, focusing on groundwater circulating in ultramafic rocks, generally as fractured reservoirs, or in sedimentary aquifers derived from their dismantling.

6.1. Comparison with Similar Hydrogeochemical Settings

In the Piedmont region, ARPA has defined the PTE NBLs in groundwater from the shallow and the deep porous aquifers, mostly located in the Po plain area at the mouth of the Lanzo valleys, with a procedure similar to that adopted in this study [48]. Both aquifers host groundwater of Mg-HCO₃ facies, due to the presence of ferromagnesian minerals in the matrix, potentially leading to high concentrations of PTEs, especially Ni and Cr. Indeed, in the shallow aquifer (GWB-S3a, sub-area GWB-S3a-A), Ni generally exceeds the TV for groundwater quality (20 $\mu\text{g/L}$). According to ARPA, the estimation of the Ni NBL in this area is not possible, as it is not sufficiently homogenous. However, the available data treatment suggests that it could reach up to 100 $\mu\text{g/L}$ [48], a value that is higher than the 95p evaluated at our site based on all the available measurements (84 $\mu\text{g/L}$), and similar

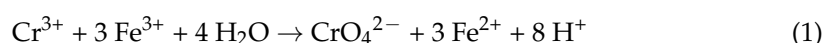
to the maximum concentration recorded (109 µg/L). The presence of Cr and Cr VI has been assessed too, but the estimation of their NBLs is complicated by the presence of a clear anthropogenic input. In the deep aquifer (GWB-P2), the two MSs located closer to the study area record Cr concentrations reaching up to 50 µg/L, and traces of Cr VI (above the LOD of 5 µg/L). In addition, ARPA evaluates the presence of Mn in groundwater. At the regional scale and in shallow aquifers, this metal shows high and variable mean contents that can reach up to 3000 µg/L. As its behaviour in solution is determined by its oxidation state and by the mobilisation processes, it is not possible to calculate an NBL due to the high spatial and temporal variability of the monitoring data. However, at the mouth of the Lanzo valleys, one station reaches concentrations higher than 200 µg/L in historical data (2005–2009) [48]. Even in this case, the maximum concentration from all the available measurements (92.1 µg/L) could therefore be justified.

In Italy, ophiolite outcrops are common in the Alpine–Apennine chain, as these are the remnants of the Ligurian–Piedmontese basin of Jurassic age [24]. In these areas, studies on the abundance of Cr and Ni in groundwater suggest that serpentinite is a source of PTE contamination of non-anthropogenic origin [49]. A recent study [50] reports and re-interprets groundwater hydrochemistry and PTE concentrations of 598 samples from five areas where variably serpentinised ultramafic rocks outcrop. As this database is available, we extracted the results of the groundwater analyses with nitrate concentrations < 37.5 mg/L and performed a descriptive statistical treatment (Table 8).

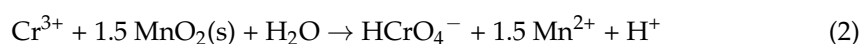
Table 8. Descriptive statistics of the PTE concentrations in Italian groundwater (in µg/L) [50] unaffected by anthropogenic contamination (i.e., with nitrate concentrations < 37.5 mg/L).

		Cr	Cr VI	Fe	Mn	Ni
N	Valid	541	96	494	474	445
	Missing	18	463	65	85	114
	Mean	7.58	15.26	25.78	2.93	13.73
	Median	4.00	12.00	8.00	0.00	5.40
	Mode	2.00	3.00	0.00	0.00	0.00
	Std. Deviation	9.71	14.64	72.36	27.80	23.01
	Skewness	2921.23	1718.94	8321.03	19147.22	4701.43
	Kurtosis	11297.90	4002.48	91757.03	392675.03	35534.60
	Minimum	0.02	0.05	0.00	0.00	0.00
	Maximum	73.00	73.00	948.00	579.00	259.60
Percentiles	25	2.00	3.00	0.000	0.00	1.15
	50	4.00	12.00	8.00	0.00	5.40
	75	9.00	21.00	19.00	0.77	18.00
	95	28.90	42.75	127.00	5.98	52.77
	99	46.17	73.00	304.05	51.10	121.16

The 95p values calculated for our study site are between the 95p and the 99p values of the Italian dataset, for Cr and Ni, and are lower than the 95p for Cr VI. However, our Fe and Mn concentrations are much higher than the 99p values of the above dataset, but lower than the maximum values reported there [50]. In the paper, the authors discuss the potential role played by Fe³⁺ included in serpentinite as an oxidising agent for Cr³⁺, following the reaction:



Based on geochemical modelling, this reaction would more accurately describe the formation of the chromate ion than the generally acknowledged reaction using Mn oxide [9,51]:



The discussion about the processes involved in the formation of Cr VI is out of the scope of this paper. However, it should be noted that, during the characterisation of the

Balangero remediation site, soils were found to contain abundant Mn oxides, especially close to the station APP127 (FGD).

Studies on groundwater contamination by Cr VI of geogenic origin are very numerous worldwide [50], ranging from simple characterisation, to statistical data treatment, analysis of correlations with other parameters, modelling of the solubilisation process and evaluation of the potential human health impact. Although the complete review of these studies is not within the scope of this paper, some of them show strong similarities with our study case and are therefore summarised below.

A thorough statistical study on the presence of Cr and Cr VI in drinking waters from California is reported by [52]. This is attributed to the presence of ultramafic and serpentinite outcrops, and to soils and sediments derived from their erosion. The more relevant results of their study are:

1. the excellent linear correlation between Cr and Cr VI, with a slope close to one. Results of over 918 datapoints indicate that $90 \pm 1\%$ of Cr is in the Cr VI form, reaching concentrations very similar to those of our study site (Figure 4);
2. the more frequent presence and the higher Cr VI concentrations found in alkaline waters ($\text{pH} > 8$) with respect to neutral or acidic waters. This is in agreement with the experimental results showing that Cr VI can be desorbed from mineral surfaces at a pH higher than 7.5;
3. the more frequent presence and the higher Cr VI concentrations found in oxic waters ($\text{O}_2 > 0.5 \text{ mg/L}$) with respect to reducing waters;
4. at comparable oxic conditions, the more frequent presence and the higher Cr VI concentrations found in deeper and older waters;
5. the negative correlation of Cr VI with other PTEs, such as Fe^{2+} , Mn^{2+} and Ni^{2+} , which are soluble at low redox potential but less soluble in oxic conditions. The negative correlation between Cr VI and Ni is also found at our study site ($N = 67$; $r = -0.33$; $p < 0.01$).

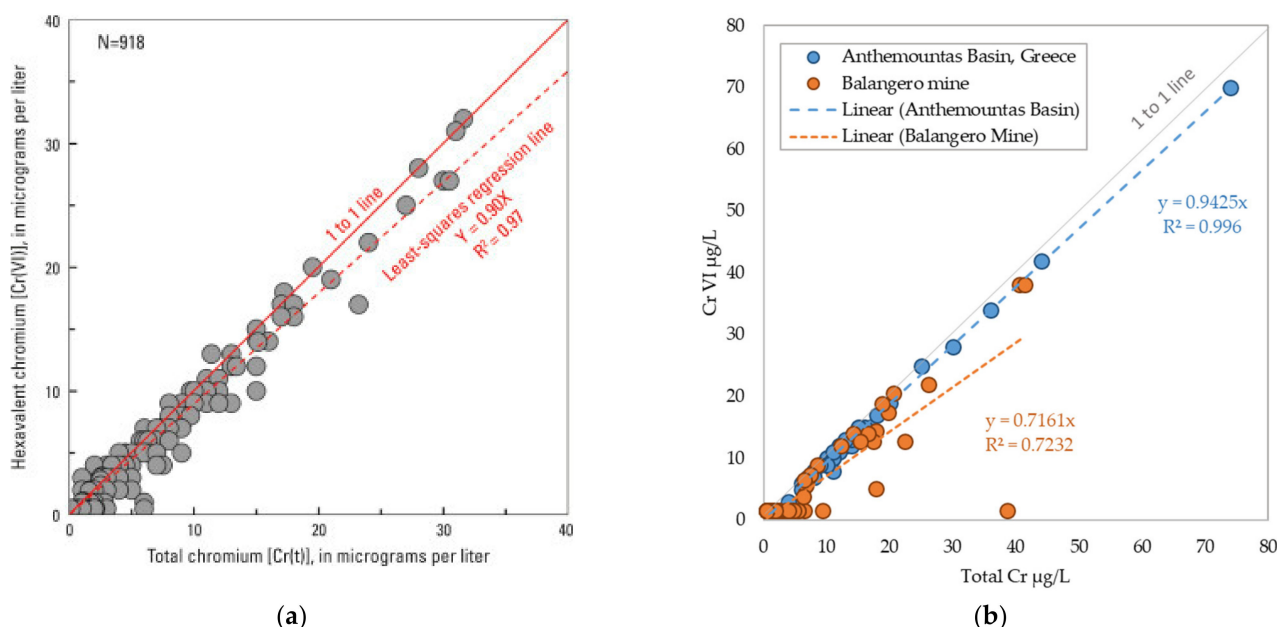


Figure 4. Relationship between Cr and Cr VI: (a) in drinking waters from California [52]; (b) in waters from the Anthemountas Basin, Greece [9] and at our study site (regression calculated using the total number of PTE measurements, including ND).

The significant correlation between Cr and Cr VI is also reported for groundwater from the Anthemountas Basin in Greece [9], reaching even higher concentrations with respect to those observed at our study site (Figure 4).

In Turkey, PTEs were analysed in an area characterised by the presence of ophiolites and of an ophiolitic mélange, sampled during the wet and the dry season [19]. These waters display E.C., dissolved oxygen and Mg-HCO₃ hydrochemical facies comparable to our study site, despite an even higher pH. The maximum concentrations recorded of Cr (11.3 µg/L), Ni (36.1 µg/L) and Zn (98.6 µg/L) are lower, whereas those of Fe (1018 µg/L) and Mn (78.6 µg/L), which are higher in the dry season, are comparable to the 95p values calculated at our study site.

High PTE concentrations are common in mining environments, especially when solutions are acidic. The processes governing the chemistry of these solutions are well known and identified under the broad name of acid mine drainage [21]. More recently, studies have addressed solutions enriched in sulphates and PTEs but at circumneutral pH (neutral mine drainage) [53,54]. Generally, the acidity related to the dissolution of sulphides in oxic environments is buffered by the host rock minerals, particularly carbonates but also silicates. However, the chemistry of the solution reflects complex processes that include the precipitation of Fe oxy-hydroxides, the co-precipitation or adsorption of other trace metals, the precipitation of Fe sulphate or gypsum and CO₂ degassing [55]. An example of such studies is reported for the Hitura mine (Finland) [20], exploiting an Fe, Ni and Cu sulphide deposit (mainly of pentlandite, chalcopyrite and pyrrhotite) hosted in serpentinite. The paper compares some parameters measured in mine waters, groundwater unaffected by mining activities and water circulating in the mine waste dumps. Uncontaminated groundwater is of Ca-HCO₃ facies, turning to Mg-SO₄ facies with increasing contamination. Low sulphates and circumneutral pH characterise unaffected waters that nevertheless show elevated Fe (mean 970 µg/L) and Mn (mean 80 µg/L) concentrations, attributed to the natural background of the area. These Fe and Mn values are comparable with the 95p values calculated for our study area.

6.2. Proposed NBLs

In Section 5.5, the percentiles that can be used as NBLs have been evaluated alternately by closely following the indications of guidelines [22] (i.e., using the MS representative values, Table 6), or by using all the available measurements (Table 7), having checked that the distribution for each element (except for Fe) can be normalised. We have also evidenced two MSs that are characterised by very high Fe and Mn concentrations due to their low redox potential. At the end of this discussion, we consider that these two stations should not be included in the evaluation of the NBLs for the following reasons:

- APP127 (FGD) was monitored from 2015 for its elevated Mn contents (Table S3). It is located in an area where, for natural reasons, abundant Mn oxides are present. FGD is characterised by a low permeability that likely prevents the diffusion of atmospheric oxygen from the surface and permits the establishment of low redox conditions, favouring the solubilisation of Fe and Mn from the matrix;
- APF140 (SERP) was only sampled once and, according to the field notes, could not be adequately purged. The elevated Fe and Mn concentrations could therefore be related to the presence of stagnant water.

Regarding the percentiles to be used as NBLs, the choice also depends on the number of MSs or measurements. If ND values are considered, the 95p can be used to estimate the NBLs, whereas if ND values are eliminated, the amount of available data should be taken into account. The guidelines suggest to select a probability level lower than $1-1/N$ (i.e., adopt the 90p when more than 10 datapoints are available; adopt the 95p when more than 20 datapoints are available; adopt the 99p when more than 100 datapoints are available). Therefore, if considering the MS representative values, only Cr and Ni would have enough data to allow for the use of the 95p, whereas for the other PTEs, the 90p (or even a lower percentile for Cr VI) should be used. By contrast, if using all the available measurements, the 95p could be used for all the PTEs, excluding Fe and Mn where the 90p should be used.

Considering Cr, if the two stations with low redox potential are excluded, the 95p values do not change much between the two calculation methods (from 38.7 to 39.3 µg/L),

and do not exceed the TV for groundwater quality (50 µg/L) [15]. The 95p for Cr VI is independent from the dataset used (38.1 µg/L) and largely exceeds the regulatory limits (5 µg/L). Total Cr and Cr VI contents are significantly correlated both if considering the MSs (N = 29; $R^2 = 0.92$; $p < 0.01$) or the full dataset (N = 67; $R^2 = 0.72$; $p < 0.01$), with the slope of the regression line close to one, indicating that all the Cr in solution is hexavalent Cr (Figure 4). This is in agreement with the literature data and supports the natural origin of this element.

Co, if the MS APP127 (FGD) is eliminated from the dataset, is always < LOD and no NBL can be calculated for this element. However, based on the available information on this MS, a natural origin of this element can be inferred. Indeed, Mn oxides strongly adsorb Co and are abundant in soils near this station.

Considering Ni, the concentrations measured in the study area are comparable with those reported in the literature. Its natural origin is suggested by the negative correlation with Cr VI, and by the assessed presence of Ni in groundwater from the Po plain aquifers, at the mouth of the Lanzo valleys. The calculated 95p values vary from 66.9 µg/L (using the MS representative values) to 84 µg/L (using all the measurements), and always exceed the TV of 20 µg/L. However, both 95p values are lower than the NBL suggested for the sector of the Po plain aquifer at the mouth of the Lanzo valleys (> 100 µg/L) [48].

The 95p values substantially differ (Tables 6 and 7) for Mn (from 22 to 71.3 µg/L), Fe (from about 330 to 630 µg/L) and Zn (from 213.5 to 307 µg/L) according to the dataset used for the evaluation. In addition, while Zn 95p values are always lower than the TV (3000 µg/L), Fe values are always higher (200 µg/L) and Mn values change from lower to higher (50 µg/L). Literature data on ultramafic rocks characterised by the presence of metallic ores, especially sulphides, indicate that groundwater concentrations in this range are commonly observed, deriving from natural water–rock interactions (i.e., neutral mine drainage). The weathering process is further enhanced in mine waste dumps, where the fractured and crushed rock has a higher surface area in contact with percolating meteoric waters.

In the investigated area, the use of the median concentration as the representative value for the MSs sampled more than once [22] involves discarding half of the data, and in particular the higher concentrations. This approach can be justified when wanting to exclude from the dataset those concentrations that could be partly affected by anthropogenic contamination. However, it is less suitable when wanting to evaluate the highest concentrations that can be naturally reached in a peculiar hydrogeochemical context such as the one investigated. A too conservative assessment of the NBLs would result in frequent overrunning of these values, initially causing unjustified alarm, and possibly leading to an underestimation of potential anthropogenic contamination processes or of the decline over time of groundwater quality. An alternative approach, once the normalisable distribution of the measurements at each station is verified, would be to use as representative the 95p instead of the median values. However, this approach cannot be adopted at our study site, as the MSs were sampled irregularly and the available measurements are not numerous enough.

Therefore, to estimate NBLs, we propose to use all the available measurements, as this dataset is more representative of the high concentrations that can naturally occur at the study site. More specifically, we propose to adopt:

- the 95p values for Cr, Ni and Mn, where Ni and Mn will exceed the TVs for groundwater quality [22];
- the 90p values for Fe and Zn, which will not exceed the TVs.

Finally, concerning Cr VI, the 95p can be used. However, it should be noted that the detectable concentrations are found in only six MSs, mostly located at the foothills of the mountain. Therefore, this NBL cannot be adopted for the full investigated area, that also includes the populated BPA.

These NBLs are summarised in Table 9. As the case study is classified as B (adequate spatial dimension, inadequate temporal dimension), with a number of stations of > 25 and

a surface extension of > 700 m², these NBL estimates are considered to have a medium confidence level (except for Cr VI) [33].

Table 9. Proposed natural background levels (NBLs) for PTEs in the study area. These correspond to the 95p values calculated for all the available measurements, excluding the two MSs with low redox potential (for Cr, Cr VI, Ni and Mn), and to the 90p values for Fe and Zn. In bold, the NBLs exceeding the TVs [15]. For Cr VI, the NBL is not representative of the BPA.

	Percentile	Proposed NBL in µg/L
Cr	95p	39.3
Cr VI	95p	38.1 *
Co	-	ND
Ni	95p	84
Mn	95p	71.36
Fe	90p	58.4
Zn	90p	232.2

* For Cr VI, the NBL is not representative of the BPA.

7. Conclusions

In this study, we illustrated the procedure followed to derive PTE concentration values for Cr (total and hexavalent), Ni, Mn, Fe and Zn that can reasonably represent the NBLs for the former Balangero asbestos mine, a “Contaminated Site of National Interest”. This area is characterised by the presence of ferromagnesian rocks, mainly serpentinite, and of sediments derived from their dismantling. In addition, metal ores (Fe, Ni and Co oxides, sulphides and alloys, also associated with other PTEs) are present, both disseminated and in veins. Therefore, the high groundwater PTE contents derive from both the weathering of ultramafic rocks, accounting especially for Cr, Cr VI and Ni, and the weathering of the metal ores, likely contributing Fe, Mn and Zn. This process is known as neutral mine drainage and is testified by increased sulphate contents and electrical conductivities, but with a circumneutral pH of the solutions.

The methodology used followed the Italian guidelines for NBL assessment, but some adjustments were required to take into account the complex (hydro)geology of the area and to better exploit all the available dataset. In particular, the guidelines recommend using the median as a representative concentration for each monitoring station. However, this involves discarding half of the measurements, and in particular the higher concentrations, thus resulting in too conservative estimates that are unable to represent this peculiar natural setting. Using, instead, all the available measurements and the recommended statistical evaluation, the derived NBLs were: Cr = 39.3, Cr VI = 38.1, Ni = 84, Mn = 71.36, Fe = 58.4, Zn = 232.2 µg/L. These values were compared with the concentrations reported in the literature for groundwater circulating in similar geological settings to support the conclusion on their natural origin.

The proposed NBLs were discussed with the authorities and were accepted as a preliminary assessment. To increase the confidence level of the estimates, in particular the temporal consistency of the dataset, further monitoring campaigns are foreseen in the coming years, targeting those MSs that exceed the TVs for Cr, Cr VI, Ni, Fe and Mn. The availability of a larger number of measurements will allow a better evaluation of the possible presence of trends in time and for finding more statistically sound NBL values. These will be again compared with data from the literature, and possibly be used for geochemical modelling of the water–rock interaction process.

Despite the positive outcome of this investigation, the results highlight the need to rethink the method indicated in the guidelines to define the MS representative concentrations. For example, different percentiles than the median could be recommended based on both the distribution and relative standard deviation of the measurements. Further discussion is needed in the scientific community about this topic, based on case studies such as the one presented, for the definition of more representative NBLs in naturally enriched environmental settings.

Supplementary Materials: The following are available online at <https://www.mdpi.com/2073-4441/13/5/735/s1>, Figure S1: Stiff diagrams. Colours of the polygons refer to the hydrogeological formation: red = SL; green = SERP; yellow = FGD; blue = BPA, Figure S2: Boxplots and normal Q–Q plots of the MS representative values: (a) total Cr; (b) Cr VI; (c) Ni; (d) Mn; (e) Fe; (f) Zn, Figure S3: Frequency histograms of the MS representative values (in µg/L), Figure S4: Frequency histograms of the total available measurements, including ND. Concentrations are in µg/L, Table S1: Physico-chemical parameters measured in the field, analytical results for major ions and charge balance error (%). GW = groundwater; SW = spring water; SL = Sesia–Lanzo; SERP = serpentinites; FGD = fluvioglacial deposits; BPA = Balangero Plain aquifer, Table S2: Minor and trace elements. Values in bold exceed the regulatory guidelines. GW = groundwater; SW = spring water; SL = Sesia–Lanzo; SERP = serpentinites; FGD = fluvioglacial deposits; BPA = Balangero Plain aquifer, Table S3: Total number of measurements of PTE concentrations available for the evaluation of the NBLs. Values in bold exceed the regulatory limits for groundwater quality, Table S4: Results of the trend analysis conducted for the MSs APP126 (a) and APE031 (b), Table S5: Results of the Shapiro–Wilk tests to evaluate the normal or lognormal distribution of the representative PTE values for each MS, Table S6: Results of the statistical tests to evaluate the presence of normal or lognormal distribution of the total number of PTE measurements.

Author Contributions: Conceptualisation, E.S. and M.B.; Data curation, E.L. and E.P.; Formal analysis, A.M. and J.-R.M.; Funding acquisition, M.B.; Investigation, E.S. and E.P.; Methodology, E.S., A.M. and J.-R.M.; Supervision, M.B.; Visualization, E.L. and E.P.; Writing—original draft, E.S.; Writing—review and editing, M.B., A.M. and J.-R.M. All authors have read and agreed to the published version of the manuscript.

Funding: This research was supported by R.S.A. srl with funds from the Italian Ministry of the Environment, Land and Sea.

Institutional Review Board Statement: Not applicable.

Informed Consent Statement: Not applicable

Data Availability Statement: The data presented in this study are available in the article and in the supplementary material.

Acknowledgments: Authors wish to acknowledge the constructive comments and the collaborative attitude of the ARPA, ISPRA and Piedmont region officers during the characterisation procedure, which contributed to achieving the goals of this research.

Conflicts of Interest: The authors declare no conflict of interest.

References

1. Pourret, O.; Hursthouse, A. It's time to replace the term "heavy metals" with "potentially toxic elements" when reporting environmental research. *Int. J. Environ. Res. Public Health* **2019**, *16*, 4446. [CrossRef] [PubMed]
2. Bradl, H.; Kim, C.; Kramar, U.; StÜben, D. *Heavy Metals in the Environment: Origin, Interaction and Remediation*; Elsevier: Amsterdam, The Netherlands, 2005; ISBN 9780120883813.
3. Meybeck, M. Heavy metal contamination in rivers across the globe: An indicator of complex interactions between societies and catchments. *IAHS-AISH Proc. Rep.* **2013**, *361*, 3–16.
4. Zheng, S.; Zheng, X.; Chen, C. Leaching Behavior of Heavy Metals and Transformation of Their Speciation in Polluted Soil Receiving Simulated Acid Rain. *PLoS ONE* **2012**, *7*, 1–7. [CrossRef] [PubMed]
5. World Health Organisation. Volume 1 Recommendations. In *Guidelines for Drinking Water Quality*, 2nd ed.; WHO: Geneva, Switzerland, 1993; ISBN 924154460.
6. BRIDGE Background cRiteria for the IDentification of Groundwater Thresholds. Available online: <http://nfp-at.eionet.europa.eu/irc/eionet-circle/bridge/info/data/en/index.htm> (accessed on 1 March 2021).
7. Vivona, R.; Preziosi, E.; Madé, B.; Giuliano, G. Occurrence of minor toxic elements in volcanic-sedimentary aquifers: A case study in central Italy. *Hydrogeol. J.* **2007**, *15*, 1183–1196. [CrossRef]
8. Viaroli, S.; Cuoco, E.; Mazza, R.; Tedesco, D. Dynamics of natural contamination by aluminium and iron rich colloids in the volcanic aquifers of Central Italy. *Environ. Sci. Pollut. Res.* **2016**, *23*, 19958–19977. [CrossRef]
9. Kazakis, N.; Kantiranis, N.; Voudouris, K.S.; Mitrakas, M.; Kaprara, E.; Pavlou, A. Geogenic Cr oxidation on the surface of mafic minerals and the hydrogeological conditions influencing hexavalent chromium concentrations in groundwater. *Sci. Total Environ.* **2015**, *514*, 224–238. [CrossRef]

10. Rotiroti, M.; Bonomi, T.; Sacchi, E.; McArthur, J.M.; Jakobsen, R.; Sciarra, A.; Etioppe, G.; Zanotti, C.; Nava, V.; Fumagalli, L.; et al. Overlapping redox zones control arsenic pollution in Pleistocene multi-layer aquifers, the Po Plain (Italy). *Sci. Total Environ.* **2021**, *758*, 143646. [[CrossRef](#)] [[PubMed](#)]
11. Megremi, I.; Vasilatos, C.; Vassilakis, E.; Economou-Eliopoulos, M. Spatial diversity of Cr distribution in soil and groundwater sites in relation with land use management in a Mediterranean region: The case of C. Evia and Assopos-Thiva Basins, Greece. *Sci. Total Environ.* **2019**, *651*, 656–667. [[CrossRef](#)] [[PubMed](#)]
12. Barceloux, D.G.; Barceloux, D. Chromium. *J. Toxicol. Clin. Toxicol.* **1999**, *37*, 173–194. [[CrossRef](#)]
13. GWD Directive 2006/118/EC of the European Parliament and of the Council of 12 December 2006 on the protection of groundwater against pollution and deterioration. *Off. J. Eur. Union* **2006**, *L372*, 19–31.
14. WFD Directive 2000/60/EC of the European Parliament and of the Council of 23 October 2000 establishing a framework for Community action in the field of water policy. *Off. J. Eur. Union* **2000**, *L327*, 1–73.
15. D. Lgs n. 152/2006. Norme in materia ambientale. *Gazz. Uff. Ser. Gen.* **2006**, *88*, 592. Available online: https://www.minambiente.it/sites/default/files/dlgs_03_04_2006_152.pdf (accessed on 1 March 2021).
16. Rotiroti, M.; Di Mauro, B.; Fumagalli, L.; Bonomi, T. COMPSEC, a new tool to derive natural background levels by the component separation approach: Application in two different hydrogeological contexts in northern Italy. *J. Geochemical Explor.* **2015**, *158*, 44–54. [[CrossRef](#)]
17. Preziosi, E.; Giuliano, G.; Vivona, R. Natural background levels and threshold values derivation for naturally As, V and F rich groundwater bodies: A methodological case study in Central Italy. *Environ. Earth Sci.* **2010**, *61*, 885–897. [[CrossRef](#)]
18. De Caro, M.; Crosta, G.B.; Frattini, P. Hydrogeochemical characterization and Natural Background Levels in urbanized areas: Milan Metropolitan area (Northern Italy). *J. Hydrol.* **2017**, *547*, 455–473. [[CrossRef](#)]
19. Güler, C.; Thyne, G.D.; Tala, H.; Yjldjrjm, Ü. Processes governing alkaline groundwater chemistry within a fractured rock (Ophiolitic mélange) aquifer underlying a seasonally inhabited headwater area in the aladallar range (Adana, Turkey). *Geofluids* **2017**, *2017*, 13–15. [[CrossRef](#)]
20. Heikkinen, P.M.; Korkka-Niemi, K.; Lahti, M.; Salonen, V.P. Groundwater and surface water contamination in the area of the Hitura nickel mine, Western Finland. *Environ. Geol.* **2002**, *42*, 313–329.
21. Blowes, D.W.; Ptacek, C.J.; Jambor, J.L.; Weisener, C.G. The Geochemistry of Acid Mine Drainage. In *Treatise on Geochemistry*; Holland, H.H., Turekian, K.K., Eds.; Elsevier: Amsterdam, The Netherlands, 2003; pp. 149–204. ISBN 9780080437514.
22. ISPRA. Linee guida per la determinazione dei valori di fondo per i suoli e le acque sotterranee, Delibera del Consiglio SNPA. In *Seduta del 14.11.2017. Doc. n. 20/2017*; ISPRA: Rome, Italy, Manuali e Linee Guida 174/2018; 2018; ISBN 978-88-448-0880-8. Available online: https://www.isprambiente.gov.it/files2018/pubblicazioni/manuali-linee-guida/MLG_174_18.pdf (accessed on 1 March 2021).
23. Piccardo, G.B. The Lanzo peridotite massif, Italian Western Alps: Jurassic rifting of the Ligurian Tethys. *Geol. Soc. London Spec. Publ.* **2010**, *337*, 47–69. [[CrossRef](#)]
24. Piccardo, G.B.; Padovano, M.; Guarnieri, L. The Ligurian Tethys: Mantle processes and geodynamics. *Earth Sci. Rev.* **2014**, *138*, 409–434. [[CrossRef](#)]
25. Ferraris, C.; Compagnoni, R. Metamorphic evolution and significance of a serpentinitized peridotite slice within the Eclogitic Micaschist Complex of the Sesia-Zone (Western Alps, Italy). *Schweizerische Mineralogische und Petrographische Mitteilungen* **2003**, *83*, 3–13.
26. Comune di Balangero Piano Regolatore Comunale Generale. Available online: <http://www.comune.balangero.to.it/Home/Menu?IDDettaglio=135816> (accessed on 19 February 2021).
27. Rossetti, P.; Zucchetti, S. Early-alpine ore parageneses in the serpentinites from the Balangero asbestos mine and Lanzo Massif (Internal Western Alps). *Rend. Della Soc. Ital. Mineral. Petrol.* **1988**, *43*, 139–149.
28. Rossetti, P.; Zucchetti, S. Occurrence of native iron, Fe-Co and Ni-Fe alloys in the serpentinite from the Balangero asbestos mine (Western Italian Alps). *Ofioliti* **1988**, *13*, 43–56.
29. Castelli, D.; Rossetti, P. Sulphide-arsenide mineralization in rodingite from the Balangero mine (Italian Western Alps): Hydrothermalism related to metamorphic fluids. In *Proceedings of the Giornata di Studio in Ricordo Del Prof. Stefano Zucchetti*, Turin, Italy, 12 May 1994; pp. 103–110.
30. Castelli, D.; Rolfo, F.; Rossetti, P. Petrology of ore-bearing rodingite veins from the Balangero asbestos mine (Western Alps). *Boll. Mus. Regionale Sci. Nat. Torino* **1995**, *13*, 153–189.
31. Groppo, C.; Compagnoni, R. Metamorphic veins from the serpentinites of the Piemonte Zone, western Alps, Italy: A review. *Period. Mineral.* **2007**, *76*, 127–153.
32. Zucchetti, S.; Mastrangelo, F.; Rossetti, P.; Sandrone, R. Serpentinization and metamorphism: Their relationships with metallogeny in some ophiolitic ultramafics from the Alps. In *Proceedings of the Zuffar' Days Symposium*, Cagliari, Italy, 10–15 October 1988; pp. 137–159.
33. Ferrante, D.; Mirabelli, D.; Silvestri, S.; Azzolina, D.; Giovannini, A.; Tribaudino, P.; Magnani, C. Mortality and mesothelioma incidence among chrysotile asbestos miners in Balangero, Italy: A cohort study. *Am. J. Ind. Med.* **2020**, *63*, 135–145. [[CrossRef](#)] [[PubMed](#)]

34. Paglietti, F.; Gennari, F.; Giangrasso, M. The asbestos extraction in the Balangero mine: Environmental consequences. In Proceedings of the Goldschmidt Conference Abstracts, Davos, Switzerland, 21–26 June 2009; p. A985. Available online: <https://goldschmidtabstracts.info/abstracts/abstractView?id=2009001620> (accessed on 1 March 2021).
35. Parrone, D.; Frollini, E.; Preziosi, E.; Ghergo, S. eNaBLE, an On-Line Tool to Evaluate Natural Background Levels in Groundwater Bodies. *Water* **2020**, *13*, 74. [[CrossRef](#)]
36. APAT; CNR-IRSA. *Metodi Analitici per le Acque*; Manuali e Linee Guida 29/2003; APAT: Rome, Italy, 2003; ISBN 88-448-0083-7.
37. Pourbaix, M. *Atlas of Electrochemical Equilibria in Aqueous Solution*, 1st ed.; Pergamon Press: Bristol, UK, 1966.
38. Edmunds, W.M.; Shand, P. (Eds.) *Natural Groundwater Quality*; Blackwell Publishing: Hoboken, NJ, USA, 2008; ISBN 978-14051-5675-2.
39. Piper, A.M. A graphic procedure in geochemical interpretation of water analyses. *Trans. Am. Geophys. Union* **1944**, *25*, 914–923. [[CrossRef](#)]
40. Stiff, H.A.J. The interpretation of chemical water analysis by means of patterns. *J. Pet. Technol.* **1951**, *3*, 15–16. [[CrossRef](#)]
41. Vitale Brovarone, A.; Martinez, I.; Elmaleh, A.; Compagnoni, R.; Chaduteau, C.; Ferraris, C.; Esteve, I. Massive production of abiotic methane during subduction evidenced in metamorphosed ophiicarbonates from the Italian Alps. *Nat. Commun.* **2017**, *8*, 14134. [[CrossRef](#)] [[PubMed](#)]
42. Mann, H. Nonparametric tests against trend. *Econometrica* **1945**, *13*, 245–259. [[CrossRef](#)]
43. Kendall, M.G. *Rank Correlation Methods*, 3rd ed.; Hafner: New York, NY, USA, 1962.
44. Meals, D.W.; Spooner, J.; Dressing, S.A.; Harcum, J.B. *Statistical Analysis for Monotonic Trends*; Tetra Tech, Inc.: Fairfax, VA, USA, 2011. Available online: https://www.epa.gov/sites/production/files/2016-05/documents/tech_notes_6_dec2013_trend.pdf (accessed on 1 March 2021).
45. Sen, P.K. Estimates of the regression coefficient based on Kendall's tau. *J. Am. Stat. Assoc.* **1968**, *63*, 1379–1389. [[CrossRef](#)]
46. Shapiro, S.S.; Wilk, M.B. An analysis of variance test for normality (complete samples). *Biometrika* **1965**, *52*, 591–611. [[CrossRef](#)]
47. D'Agostino, R.B.; Belanger, A.; D'Agostino, R.B. A Suggestion for Using Powerful and Informative Tests of Normality. *Am. Stat.* **1990**, *44*, 316–321.
48. De Vos, W.; Tarvainen, T.; Salminen, R.; Reeder, S.; De Vivo, B.; Demetriades, A.; Pirc, S.; Batista, M.J.; Marsina, K.; Ottesen, R.-T.; et al. *Geochemical Atlas of Europe. Part 2—Interpretation of Geochemical Maps, Additional Tables, Figures, Maps, and Related Publications*; De Vos, W., Tarvainen, T., Eds.; Geological Survey of Finland, Espoo: Espoo, Finland, 2006; ISBN 951-690-956-6.
49. ARPA Piemonte. *Definizione dei Valori di Fondo Naturale per i Metalli Nelle Acque Sotterranee Come Previsto Dalla Direttiva 2006/118/CE e dal Decreto Legislativo 16 Marzo 2009 n.30*; ARPA Piemonte: Turin, Italy, 2012; Available online: <https://www.arpa.piemonte.it/approfondimenti/temi-ambientali/acqua/acque-sotterranee/Relazionevaloridifondosotterranee.pdf> (accessed on 1 March 2021).
50. Langone, A.; Baneschi, I.; Boschi, C.; Dini, A.; Guidi, M.; Cavallo, A. Serpentine-water interaction and chromium(VI) release in spring waters: Examples from Tuscan ophiolites. *Ophioliti* **2013**, *38*, 41–57.
51. Apollaro, C.; Fuoco, I.; Brozzo, G.; De Rosa, R. Release and fate of Cr(VI) in the ophiolitic aquifers of Italy: The role of Fe(III) as a potential oxidant of Cr(III) supported by reaction path modelling. *Sci. Total Environ.* **2019**, *660*, 1459–1471. [[CrossRef](#)]
52. McClain, C.N.; Fendorf, S.; Webb, S.M.; Maher, K. Quantifying Cr(VI) Production and Export from Serpentine Soil of the California Coast Range. *Environ. Sci. Technol.* **2017**, *51*, 141–149. [[CrossRef](#)] [[PubMed](#)]
53. Izbicki, J.A.; Wright, M.T.; Seymour, W.A.; McCleskey, R.B.; Fram, M.S.; Belitz, K.; Esser, B.K. Cr(VI) occurrence and geochemistry in water from public-supply wells in California. *Appl. Geochem.* **2015**, *63*, 203–217. [[CrossRef](#)]
54. Iribar, V. Origin of neutral mine water in flooded underground mines: An appraisal using geochemical and hydrogeological methodologies. In Proceedings of the Mine Water 2004-Proceedings International Mine Water Association Symposium, Newcastle upon Tyne, UK, 20–25 September 2004; Volume 1, pp. 169–178. Available online: https://www.imwa.info/docs/imwa_2004/IMWA2004_22_Iribar.pdf (accessed on 1 March 2021).
55. Frau, F.; Medas, D.; Da Pelo, S.; Wanty, R.B.; Cidu, R. Environmental effects on the aquatic system and metal discharge to the mediterranean sea from a near-neutral zinc-ferrous sulfate mine drainage. *Water, Air, Soil Pollut.* **2015**, *226*, 1–17. [[CrossRef](#)]